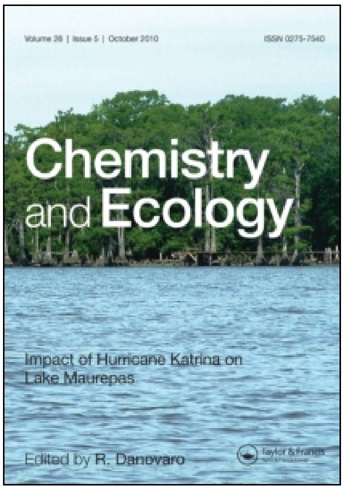

Chemistry and Ecology
Publication details, including instructions for authors and subscription information:
http://www.informaworld.com/smpp/title~content=t713455114

Application of a finite element model to the taranto sea

Isabella Scroccaro[a]; Raffaella Matarrese[b]; Georg Umgiesser[a]
[a] ISMAR-CNR-S.Polo, Venezia, Italy [b] Dip. Fisica, Università di Bari, Bari, Italy

To cite this Article Scroccaro, Isabella , Matarrese, Raffaella and Umgiesser, Georg(2004) 'Application of a finite element model to the taranto sea', Chemistry and Ecology, 20: 3, 205 — 224
To link to this Article: DOI: 10.1080/02757540410001655404
URL: http://dx.doi.org/10.1080/02757540410001655404

Chemistry and Ecology
June 2004, Vol. 20 (Supplement 1), pp. S205–S224

APPLICATION OF A FINITE ELEMENT MODEL TO THE TARANTO SEA

ISABELLA SCROCCARO[a], RAFFAELLA MATARRESE[b] and GEORG UMGIESSER[a,*]

[a]*ISMAR-CNR-S.Polo, 1364-30125 Venezia, Italy;* [b]*Dip. Fisica, Università di Bari, V. Amendola, 173-70100 Bari, Italy*

The two-dimensional finite element model SHYFEM is used to study the hydrodynamics and variability of temperature and salinity of the Taranto Sea. The model is calibrated and validated with experimental data collected by local research organizations during *in situ* campaigns from 2000 to 2001. A 1-year simulation was set up taking into account different forcings such as tide, meteorological data, and fresh water discharges. The results show that the temperature variability is well reproduced in the basin and salinity is mainly determined by the contribution of fresh water inflow and evaporation process. The final results from the model are in good agreement with the measured data and this study will be a first step towards a water quality model for the Taranto Sea.

Keywords: Finite element model; Numerical simulations; Coastal ecosystems; Taranto Sea

1 INTRODUCTION

The Taranto Sea represents a coastal marine ecosystem that has been gradually modified by mankind. It is situated in the Ionian Sea in southern Italy and it is composed of two parts: the Mar Grande and the Mar Piccolo (see Fig. 1).

The Mar Grande covers an area of 35 km^2 with a maximum depth of about 35 m and an average depth of about 15 m. It connects with the Ionian Sea through two openings. The first one is about 1 km wide and is situated in the southern part of the basin, between S. Paolo island and Capo S. Vito. The second one is about 100 m wide, located in the north-western part of the Mar Grande near Punta Rondinella.

The Mar Piccolo of Taranto has a total surface area of 20.72 km^2 structured in two shelves, the 'First Seno' and the 'Second Seno'. The maximum depth is about 15 m for the First Seno and about 10 m for the Second Seno. The average depth of the two subsystems is about 5 m (Pastore, 1993). The Mar Piccolo is connected to the Mar Grande by two narrow channels, along the island of the old town of Taranto, the *Navigabile* channel and the *Porta di Napoli* channel.

The Mar Piccolo is characterized by the presence of about 30 submarine fresh water springs, locally called 'Citri'. The two most important ones (taken into account in this

* Corresponding author. Tel.: +39-041-5216875; Fax: +39-041-12602340; E-mail: georg.umgiesser@ismar.cnr.it

ISSN 0275-7540 print; ISSN 1029-0370 online
DOI: 10.1080/02757540410001655404

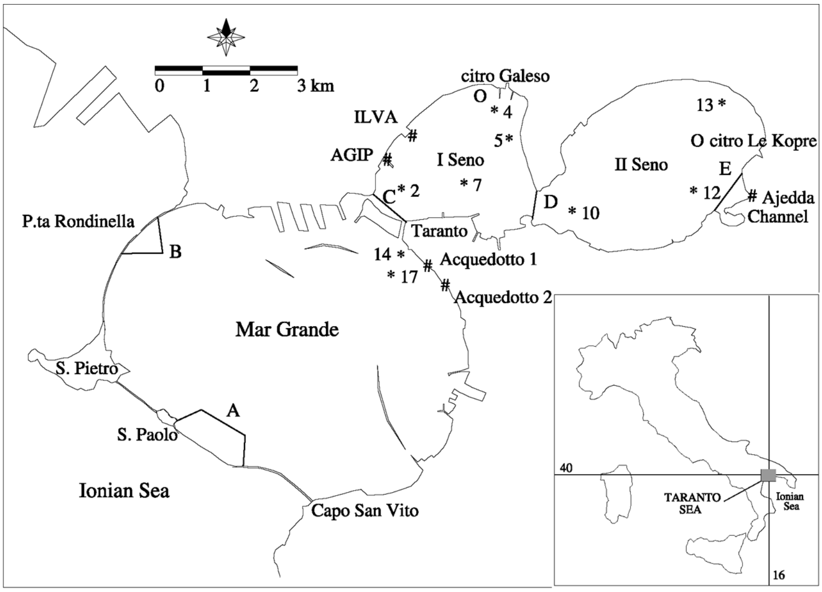

FIGURE 1 Map of the Taranto basin with the positions of the sampling stations (∗), of the submarine fresh water springs (O), of the inflow points (#) and the sections (A–E) where water fluxes are computed by the model.

study) are the citro Galeso, in the First Seno near the Galeso river, and the citro Le Kopre, in the north-eastern part of the Second Seno. Furthermore, a water pump serving the industrial plant of ILVA withdraws about 35 m^3/s from the First Seno of the Mar Piccolo.

The climate of the region is distinguished by two periods: a rainy winter period and a dry summer period, which sometimes extends into autumn. The mean annual air temperature is 16.9 °C, with minima of 9 °C in January and maxima of 25.7 °C in July. An important factor that influences the discharge of the underwater springs and hence the salinity and the environmental conditions of the Mar Piccolo is the pattern of the rainfall, which amounts to an average of 489.8 mm per annum, though rainy years alternate with dry years. This rainfall pattern determines a reduction in salinity and an increase in the development of the plankton (Vatova, 1972). The mean temperature of water is 16.9 °C for the Mar Grande and 18.3 °C for the Mar Piccolo. The average salinity of the whole volume of water is 38.11 psu for the Mar Grande, with slight monthly variations, and 36.49–36.32 psu for the Mar Piccolo. Moreover, in the Mar Grande only small differences are noted in the salinity between dry and wet years, whereas in the Mar Piccolo these differences are far more marked, especially in the surface salinity: in the First Seno it ranges between 35.99 and 35.55 psu, and in the Second Seno between 36.16 and 35.28 psu. In fact, under the abiotic aspect, the two basins of the Mar Piccolo have been considered as two different ecosystems influencing each other (Vatova, 1972).

The wind pattern of the zone presents mainly the wind from NW, prevailing during the whole year, and secondly the wind from SE and S. The typical wind speed is about 3 m/s with maximum values up to about 8–9 m/s (see Fig. 2 for reference).

Problems due to the increasing pollution from various sources are reducing the environmental quality of the Taranto Sea. In fact, it is exposed to industrial discharges and receives a considerable amount of sewage from the northern part of Taranto and from the nearby towns. For example the Ajedda Channel discharges the waste waters of eight municipalities into the Second Seno of the Mar Piccolo.

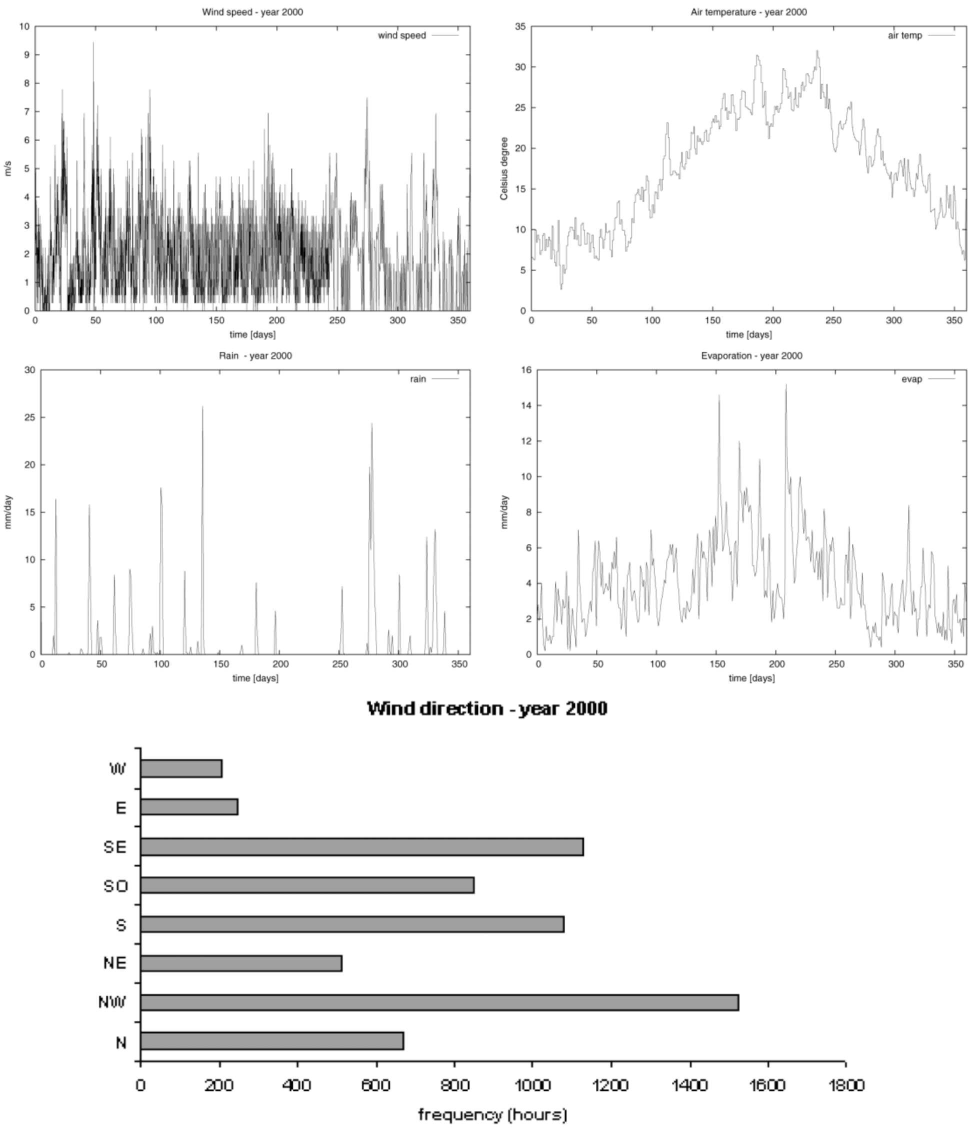

FIGURE 2 Top and center: Time series of wind speed, air temperature, rain, and evaporation for the year 2000. Bottom: Wind direction for the year 2000.

Several studies have been carried out to characterize the situation in the Taranto Sea. Vatova (1972) summarizes the hydrographic observations carried out monthly between 1962 and 1969 at five stations situated in the two Taranto seas; Strusi and Pastore (1975) evaluate by statistical analysis the physical–chemical parameters collected during the campaign from 1970 to 1971. The biological and microbiological parameters of the pollution, the conditions of benthonic populations, and the main environmental impact problems and phenomena of contamination, in particular in the sediments, have been studied by Cavallo *et al.* (1994), Cardellicchio *et al.* (1991), Tursi *et al.* (1981), respectively; the physical–chemical conditions and the particulate matter have been analyzed recently with statistical methods by Alabiso *et al.* (1997), but no previous effort has been put into the numerical modeling of the Taranto Sea.

In this article the application of the two-dimensional finite element (FE) model Shallow water Hydrodynamic FE Model (SHYFEM), developed at Institute of MARine Science (ISMAR-CNR) in Venice (Umgiesser, 1986) is presented for the Taranto Sea. The aim of this article is to investigate the variability of the temperature and salinity and the dynamics of the Taranto Sea with a modeling approach. The model SHYFEM has been successfully applied to other Italian lagoons: the Venice lagoon (Umgiesser, 1997, 2000), the Orbetello lagoon in Tuscany (Scroccaro *et al.*, 1999, 2001) and the Cabras lagoon in Sardinia (Ferrarin and Umgiesser, 2003).

In Section 2 the FE model and the simulation set-up are presented and Section 3 illustrates the results, while Section 4 draws the conclusions.

2 MATERIALS AND METHODS

2.1 The Finite Element Model

The two-dimensional FE model SHYFEM, developed at ISMAR-CNR in Venice, consists of a hydrodynamic module, especially suited for shallow water, which uses the FE method for the spatial resolution and a semi-implicit scheme for the time integration.

The FE method was developed in 1950s and has been used for hydrodynamic applications, since 1970s. This method is well suited to describe in high details areas with complicated geometry. The FE method uses a combination of linear and constant form functions to solve the unknowns of the differential equations, such as the total water depth, the water level, the velocities, and other model parameters. Details are provided in Umgiesser and Bergamasco (1995).

The model contains a dispersion module and a heat flux module that will be described below. A water quality model also exists that is coupled to the hydrodynamic model (Umgiesser *et al.*, 2003).

2.1.1 The Hydrodynamic Equations

The FE model solves the vertically integrated shallow water equations of momentum and mass:

$$
\begin{aligned}
\frac{\partial U}{\partial t} - fV + gH\frac{\partial \xi}{\partial x} + RU + X &= 0 \\
\frac{\partial V}{\partial t} - fU + gH\frac{\partial \xi}{\partial y} + RV + X &= 0 \\
\frac{\partial \varsigma}{\partial t} + \frac{\partial U}{\partial x} + \frac{\partial V}{\partial y} &= 0
\end{aligned}
$$

where ξ is the water level; h, the undisturbed water depth and $H = h + \xi$, the total water depth; g, the gravitational acceleration; t, the time; R, the bottom friction coefficient; and f is the Coriolis parameter.

U and V are the vertically-integrated velocities (total or barotropic transports):

$$
U = \int_{-h}^{\varsigma} U \,\mathrm{d}z \quad V = \int_{-h}^{\varsigma} V \,\mathrm{d}z
$$

with u and v the velocities in the x and y directions, respectively.

The terms X and Y contain all the other terms such as the wind stress, the advective non-linear terms and the horizontal turbulent diffusion terms. They read:

$$X = u\frac{\partial U}{\partial x} + v\frac{\partial U}{\partial y} - \frac{1}{\rho_0}\tau_x - A_{\mathrm{H}}\left(\frac{\partial^2 U}{\partial x^2} + \frac{\partial^2 U}{\partial y^2}\right)$$

$$X = u\frac{\partial V}{\partial x} + v\frac{\partial V}{\partial y} - \frac{1}{\rho_0}\tau_y - A_{\mathrm{H}}\left(\frac{\partial^2 V}{\partial x^2} + \frac{\partial^2 V}{\partial y^2}\right)$$

where ρ_0 is the constant density and A_{H} is the horizontal eddy viscosity.

The action of the wind on the water surface has been included in the terms X and Y through the following formula for the wind stress τ:

$$\tau_x = c_{\mathrm{d}}\rho_{\mathrm{a}}|u_{\mathrm{w}}|u_{\mathrm{w}}^x \quad \tau_y = c_{\mathrm{d}}\rho_{\mathrm{a}}|u_{\mathrm{w}}|u_{\mathrm{w}}^y$$

where c_{d} is the dimensionless drag coefficient; ρ_{a}, the density of air (1.2 kg/m^3); u_{w}^x and u_{w}^y, the components of the wind speed at a height of 10 m above the surface; and $|u_{\mathrm{w}}|$ is the modulus of the wind speed.

The friction coefficient is expressed as

$$R = \frac{g\sqrt{u^2 + v^2}}{C^2 H}$$

where the term C is the Chezy coefficient, which varies with the water depth as follows

$$C = k_{\mathrm{s}} H^{1/6}$$

where k_{s} is the Strickler coefficient.

The terms treated semi-implicitly are the pressure gradient and the Coriolis term in the momentum equation and the divergence terms in the continuity equation. The bottom friction term has been discretized fully implicitly and the terms X and Y are treated explicitly. Details are given in Umgiesser and Bergamasco (1993, 1995).

2.1.2 The Dispersion Module

The dispersion module runs in parallel with the hydrodynamic model. The equation for the dispersion of the general property A (temperature or salinity for the Taranto Sea) is:

$$\frac{\partial A}{\partial t} + u\frac{\partial A}{\partial x} + v\frac{\partial A}{\partial y} = K\left(\frac{\partial^2 A}{\partial x^2} + \frac{\partial^2 A}{\partial y^2}\right) + S$$

where $u(\partial A/\partial x)$ and $v(\partial A/\partial y)$ are the advective terms, and $K((\partial^2 A/\partial x^2) + (\partial^2 A/\partial y^2))$ are the dispersion terms with K as the constant horizontal eddy diffusivity coefficient. S represents the sources and sinks of the property A.

For the study of water temperature variability a thermal radiative term $S = Q/C$ was added to the dispersion module (Zampato *et al.*, 1998). In this way, the heat exchanges with the atmosphere are contained in the source term Q/C, where $C = c\rho V$ is the thermal capacity for volume V, with ρ, the water density; and $c = 4183$ J/kg/K is the specific heat of water.

Q is the heat flux between the atmosphere and the sea in W/m^2. Q is computed in the model as follows:

$$Q = Q_s + Q_b + Q_e + Q_h$$

where each term indicates a physical process:

- Q_s is the short wave (solar) radiation;
- Q_b is the long wave radiation;
- Q_e is the latent heat flux generated by the evaporation–condensation process;
- Q_h is the sensible heat flux generated by the conduction–convection process.

The heat provided by the solar radiation is adsorbed, transported by the water currents, and exchanged with the atmosphere by the processes indicated above, on the basis of which the temperature in the Taranto Sea is calculated by the model. Details are given in Zampato *et al.* (1998).

For the study of the salinity evolution, the term S indicates the sources and/or the sinks of the property. For the Taranto Sea these terms are represented by the fresh water inflows (river, 'citri', waste waters, rain) and evaporation.

The results of the module are the temperature and salinity distributions, expressed as mean values in the water column, due to the 2D nature of the model.

2.1.3 The Finite Element Grid

The FE model performs the computation for the unknowns on a grid formed by triangular elements, varying in form and size, that reproduces accurately the topography of the investigated area.

The transport velocities U and V are defined on the center of gravity of the triangle while the water levels ξ are defined on the vertices of the triangles. The resulting grid may be seen as a staggered grid where the unknowns are defined on different locations. Therefore, the grid resembles very much the Arakawa B-grid used in the finite difference method (i.e., water levels on the center and the velocities on the four vertices of a square). See Umgiesser *et al.* (1995) for details.

The grid for the Taranto Sea was constructed with an automatic mesh generator. It contains 4452 nodes and 8059 triangular elements, with sides of the elements varying from about 10 to about 200 m. The resulting grid is shown in Fig. 3. As it can be seen, a higher grid resolution was imposed in the areas of greater interest, such as the island of the old town of Taranto, the eastern coast of the Mar Grande, where waste water discharges exist, the zone around the water pump of ILVA, the connection area between the First Seno and the Second Seno, and near the Ajedda Channel.

The coastline and the bathymetric data used to build the grid were obtained from the 'Carta Nautica del Porto di Taranto e Mar Grande 1:20,000', provided by the Biology Department of the University of Bari. The bathymetric data, necessary for the FE model to run, have been inserted in every element.

2.2 The Simulation Set-up

The model was forced for 1 year with tide, meteorological data, and the inflows into the Taranto Sea, collected during 2000. In the same simulation the hydrodynamics, and the temperature and salinity evolution are calculated.

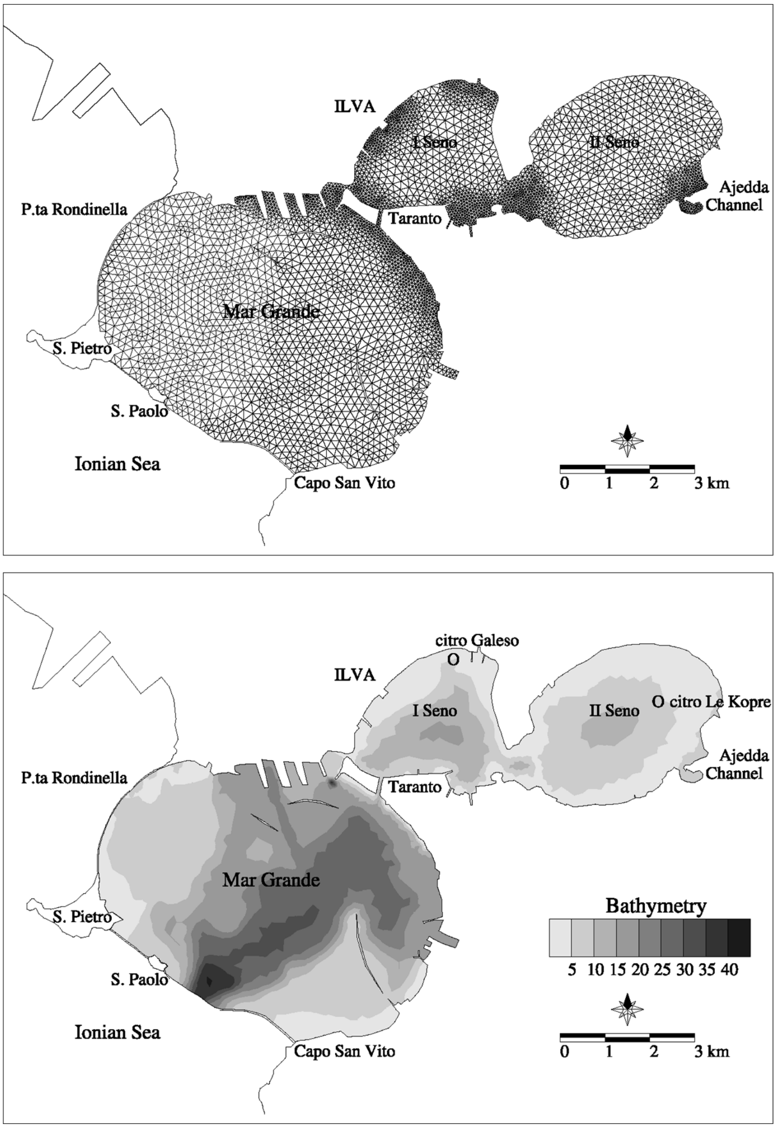

FIGURE 3 Top: Grid of the FE model SHYFEM. Bottom: Bathymetry of the investigated area, as represented by the FE model, with the positions of the submarine fresh water springs.

The tide is prescribed at the two inlets of the Mar Grande as an open boundary condition. The tidal data have been measured by a tide gauge situated on the Porta di Napoli Channel along the old Taranto island and are provided by the Servizi Tecnici Nazionali for the year 2000. Spring tides have a range of about ±0.15 m and neap tides of about ±0.08 m.

The river runoff and waste water discharge values (shown in Tab. I) come from the Biology Department of Bari University. Furthermore the Istituto Talassografico of CNR of Taranto made an *in situ* estimate of the fresh water springs discharge, presented in Table II. These inflows into the basin were kept constant. It has to be stressed that there are considerable seasonal fluctuations that may change these values intermittantly, but no experimental data are available.

TABLE I Discharge values for the Taranto Sea, with estimated values of salinity and temperature.

Inflow	*Discharge (m^3/s)*	*Salinity (psu)*	*Temperature (°C)*
Ajedda Channel	1.03	1.5–5	20
ILVA	−35	–	–
AGIP	0.2	1.5–5	20
Acquedotto 1	0.3	1.5–5	20
Acquedotto 2	0.3	1.5–5	20
Citro Galeso	0.6	1.5–5	18
Citro Le Kopre	0.1–1.2	1.5–5	18

TABLE II Comparison between the discharge estimates of the two fresh water springs.

Inflow	*Bari University (m^3/s)*	*Ist. Talassografico (m^3/s)*
Citro Galeso	0.6	0.6
Citro Le Kopre	1.2	0.1

Wind speed and direction collected by the Istituto Meteorologico *L. Ferrajolo* of Taranto were used to force the model. The station is located along the coast at about 6 km from the city of Taranto. The same station also measured the other meteorological data, necessary for the dispersion and radiative module, such as solar radiation, air temperature, relative humidity, and cloud cover. In particular the solar radiation data were obtained from heliophany data by a conversion with an empirical formula (Benincasa *et al.*, 1991). Details are given in Scroccaro *et al.* (2002b). Other inputs provided by the meteorological station for the dispersion module are rain and evaporation data.

Temperature and salinity measurements were collected by CTD probes during *in situ* campaigns for the years 2000–2001 and were used for calibration of the dispersion module. The data points consist of nine stations, two stations in the Mar Grande (14 and 17), four stations in the First Seno (2, 4, 5, and 7), and three stations in the Second Seno of the Mar Piccolo (10, 12, and 13). The positions of the sampling stations are presented in Fig. 1.

The simulation was carried out using a time step of 600 s. The model was allowed to achieve a steady state in 4 months (beginning at 1 September 1999), and then the simulation for the year 2000 starts. The bottom friction uses a constant value for the Strickler coefficient k_s of 36.

Wind data has been available from one station with an hourly frequency. This wind is used with the dimensionless drag coefficient c_d equal to $2.5 \cdot 10^{-3}$.

The simulation results consist in daily outputs of water fluxes through the sections indicated in Fig. 1, velocity, temperature, and salinity fields. More comments are given in the following section where the results are presented.

3 RESULTS AND DISCUSSION

In this section the results of the FE model are presented. The general circulation and the temperature and salinity variability are discussed for the Taranto Sea.

3.1 Hydrodynamics

The water fluxes and the velocity field in the Taranto Sea were investigated using the hydrodynamic model. Tide, wind, and inflow data were prescribed as forcings (see Tab. I for inflow values). A 1-year simulation (referring to 2000) was performed in order to describe the general features of the circulation in the Taranto Sea.

Figure 4 shows instantaneous fields of velocity. In the top panel (16 January 2000, 06:00 h), the wind blows from northwest at about 5 m/s, with outflowing tide, and in the bottom panel (2 August 2000, 15:00 h), it blows from south at about 3.3 m/s, with inflowing tide.

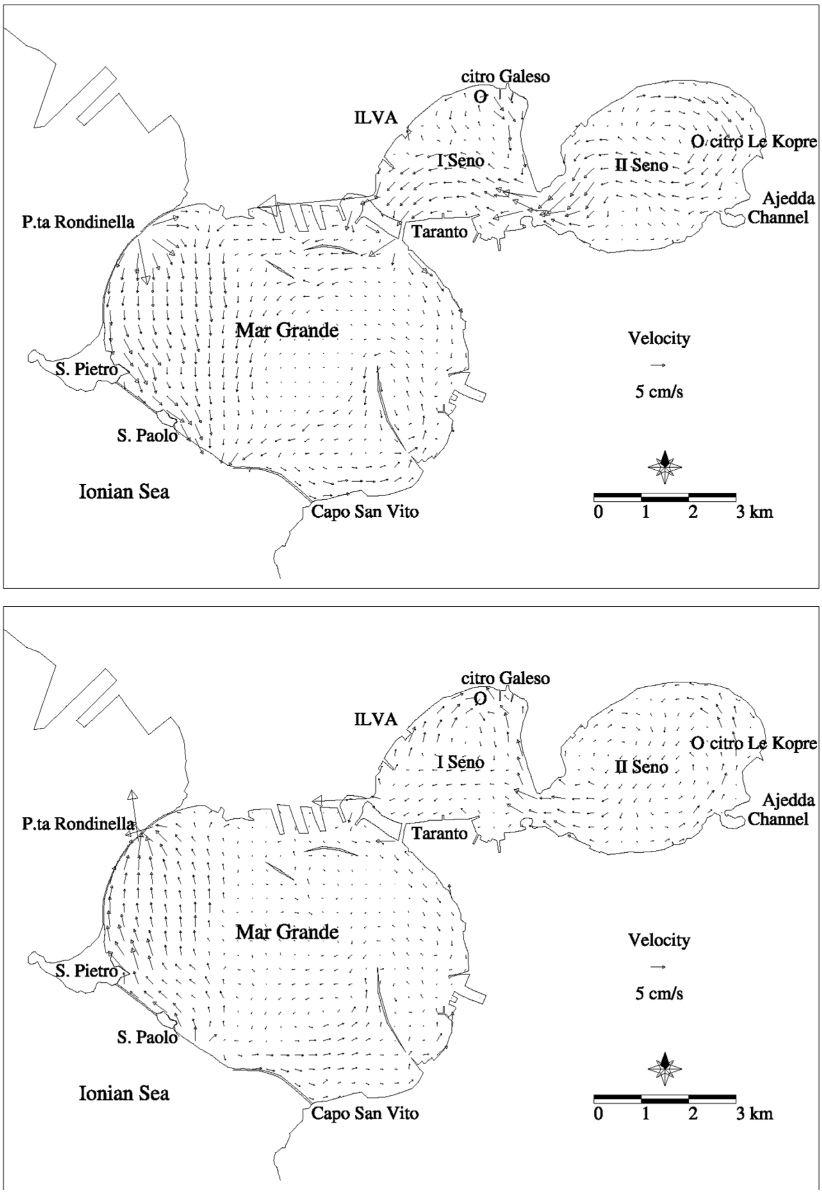

FIGURE 4 Instantaneous pictures of the velocity field in the Taranto Sea. Top: 16 January 2000, 06:00 h (wind from NW and outflowing tide). Bottom: 2 August 2000, 15:00 h (wind from S and inflowing tide).

In the Mar Grande the circulation consists of along-shore currents, which follow the direction of the wind and are modulated by the tide. The water masses from the Mar Grande enter the Mar Piccolo through the two connection channels along the island of the old city of Taranto. This flux splits up into 35% through the Porta di Napoli Channel (western channel) and 65% through the Navigabile Channel (Scroccaro *et al.*, 2002a). The formation of some gyres can be observed in the Mar Piccolo: in particular in the Second Seno a cyclonic gyre (top panel) and an anticyclonic gyre (bottom panel) are present, with low current velocities (1–5 cm/s).

In general the currents have no great energy (about 5–10 cm/s) and the maximum velocity can be observed in the two connection channels between the Mar Grande and the Mar Piccolo (up to 30–40 cm/s) and near the two openings (about 20–25 cm/s). The areas of lower hydrodynamic activity seem to be in proximity to the Ajedda Channel and on the northern side of the Mar Grande.

In a previous study the model was run with and without the fresh water springs and the discharge contributions (Scroccaro *et al.*, 2002a). The comparison of the results showed that the influence of the fresh water springs and discharges is insignificant for the hydrodynamic activity, whereas the water pump of ILVA, picking up about 35 m^3/s from the First Seno of the Mar Piccolo, has some effect on the local circulation. In particular this can be seen in the top panel of Fig. 4: the arrow near the ILVA inlet is an indication of the modified circulation due to the water pump.

In Fig. 5 the daily averaged water fluxes through the sections A–B (top panel) and C–D (bottom panel) are plotted. Positive (negative) values indicate in-going (out-going) flow. The daily averaged flux oscillates in a range of around $\pm 700\,m^3/s$, with some peaks at days 52 (about $\pm 1170\,m^3/s$), 274–275 (about ± 1030 and $1350\,m^3/s$), and 332 (about $\pm 1000\,m^3/s$), due to strong wind events (see also Fig. 2). The values for sections A and B are positive or negative depending on the direction of the wind (Scroccaro *et al.*, 2002a).

The water either enters the Mar Grande from the southern inlet (section A) and exits from Punta Rondinella (section B) or enters from Punta Rondinella and exits from the southern inlet. This behavior can be explained by looking at the mass balance of the Mar Grande: if there is no net accumulation, the water masses, that are pushed into the Mar Grande by the wind action, must leave the basin through the other inlet. Once the tidal action is filtered out (1 day averages), the fluxes through the two inlets of the Mar Grande seem to be approximately 180° out of phase, as can be seen in the top panel of Fig. 5.

On the contrary, the exchanges between the Mar Grande and the Mar Piccolo are mainly driven by the tidal action. In this case (bottom panel of Fig. 5), the wind seems to have a minor role with respect to the tide. Some peaks can still be observed that are not related to the ones of sections A and B, and the values for sections C and D are strongly reduced. In fact the fluxes range from about 10 to 50 m^3/s for section C and they oscillate between $\pm 10\,m^3/s$ for section D. The difference in the mean value between the flux through sections C and D represents the water quantity captured by the water pump of ILVA in the First Seno, plus the input of fresh water springs and discharges. Results for section E are not presented, because they are not significant.

Therefore, there are two different mechanisms that are responsible for the water exchange between the Mar Grande and the open sea and the Mar Grande and the Mar Piccolo: on one side, the wind is strongly enhancing the exchanges with the open sea; on the other hand, the wind does not have such a big influence on the exchanges with the Mar Piccolo. This can be seen from the fact that with a drag coefficient twice the actual value (corresponding to twice the momentum input through the water surface), the average discharge through section A passes from 73.52 to 87.51 m^3/s (+19%), whereas the flux through the Navigabile channel, the eastern connecting channel between Mar Grande and Mar Piccolo, changes by only 0.4 m^3/s (not shown). Even if we look at the variability of the discharge (standard

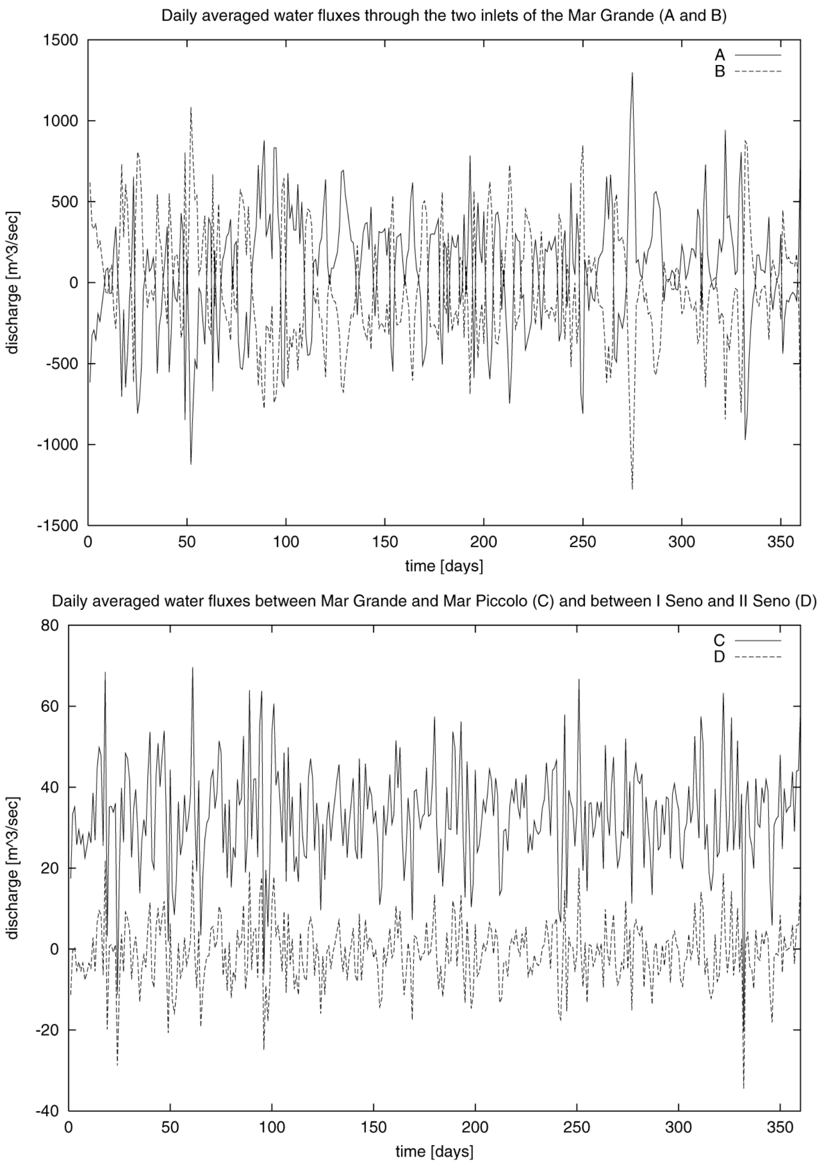

FIGURE 5 Top: Daily averaged water fluxes through the two inlets of the Mar Grande (A, B). Bottom: Daily averaged water fluxes between Mar Grande and Mar Piccolo (C) and between I Seno and II Seno of the Mar Piccolo (D).

deviation), section A passes from 286 to 403 m^3/s (+41%), whereas the flux through the Navigabile channel increases from 9.8 to 12.5 m^3/s (+26%, not shown).

It is also interesting to note that the bottom friction parameter has little effect on the exchanges of the Mar Piccolo. In fact, using a value of $k_s = 30$ for the Strickler coefficient, no significant changes in the exchange rates were found. The Mar Piccolo is therefore, hydrodynamically speaking, an open basin that is already well connected to the Mar Grande with its exchange rates mainly governed by the tidal action. These general features of the circulation in the Taranto Sea, in particular the role of tide and wind in the Mar Grande and in the Mar Piccolo, will be investigated in more detail in a successive study.

3.2 Temperature Distribution

A 1-year simulation was performed with the dispersion radiative model to simulate the temperature behavior in the Taranto Sea for the year 2000. The model was initialized with constant water temperature of 18 °C everywhere, starting from 1 September 1999. The values of 20 and 18 °C were imposed for the inflows and for the fresh water springs temperatures, respectively, as reported in Table I. Because no data were available at the two openings with the Ionian Sea, the temperature of the sampling station 14 was used for the open boundary.

In Figs. 6 and 7 the comparison of the temperature time series between the computed (continuous line) and measured data (crosses) is shown for the sampling stations (see Fig. 1). A small spatial variability can be observed in the temperature of the nine stations. The model results for stations 17 and 2 are plotted at the top, for stations 7, 4, 5, and 10 in the middle, and for stations 12 and 13 at the bottom. Results for station 14 are not presented because they are similar to station 17.

In a first simulation (Fig. 6) the results reproduced the seasonal trend of the temperature distribution for the year 2000. Minimum values in the winter period and maximum values in the summer time were correctly simulated, but the model computed higher values in the stations situated in the Mar Piccolo, especially from June to September, and lower values in January and February.

Due to the high amount of humidity present in the air, the solar radiation data were probably overestimated during summer time. Furthermore, these values were calculated from heliophany data, as provided by the meteorological station which adds some more uncertainty to the radiation data. After some sensitivity tests the solar radiation data were reduced in 20% of their original value for the period May–September, as described in Scroccaro *et al.* (2002b).

Figure 7 exhibits the model results after the calibration. The seasonal behavior, with minimum values of 8–9 °C up to maximum values of 26–27 °C, is simulated in a reasonable agreement with the temperature data. For this experiment, the root mean square error was equal to 1.37 °C, an improvement with respect to the first simulation where it was 1.74 °C.

The results show that the dispersion radiative module used in this application reproduces reasonably well the temperature variability at the sampling stations.

3.3 Salinity Distribution

Similar to the temperature, the salinity evolution was modeled for the year 2000. Figures 8 and 9 show the salinity time series computed by the model (continuous line) compared to the *in situ* data (crosses).

A value of 37 psu was prescribed as initial condition and the measurements at station 14 were used as an indication of the boundary value to impose. Since this station is already affected by the inflow of fresh water, after some calibration runs a value of 1.25 psu was added to the data in order to simulate the value of the open boundaries. With this offset the salinity in station 14 is described well (see Figs. 8 and 9). The inflow values reported in Table I were prescribed at the boundaries. After some tests, from 1.5 to 5 psu, a value of 5 psu was assigned to the salinity of the inflows.

The simulated salinity evolution is presented in Fig. 8, showing great discrepancies with the measurements. The results, especially the ones in the Mar Piccolo, exhibit lower values compared to the experimental data. An agreement is present only for the station 14 in the Mar Grande, which is not surprising since this station were used to prescribe the open boundary conditions. Also, the seasonal variability effect that can be seen in the data (higher salinity in summer due to evaporation and lower discharges) is not well reproduced by the model.

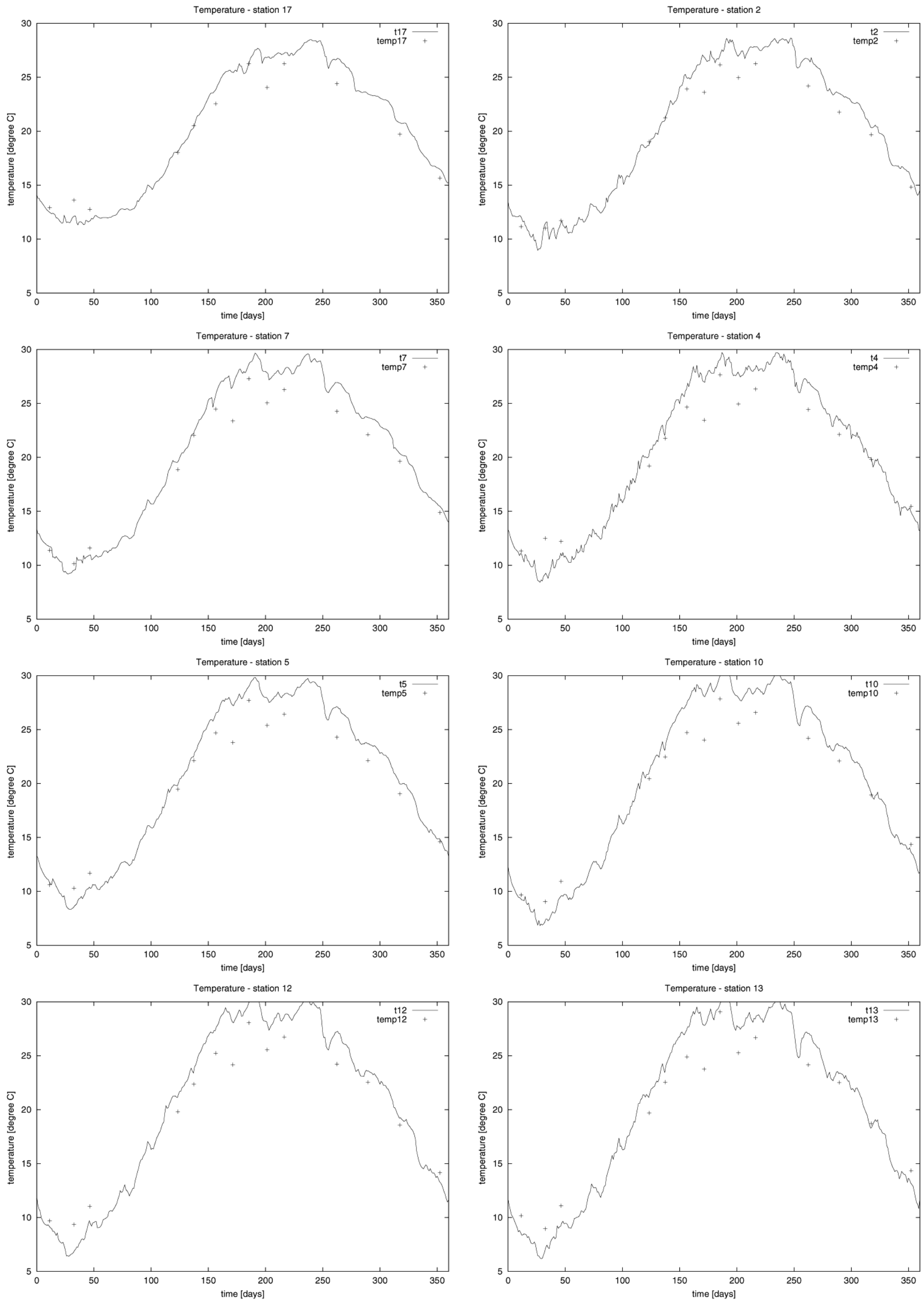

FIGURE 6 Results of the reference simulation for temperature.

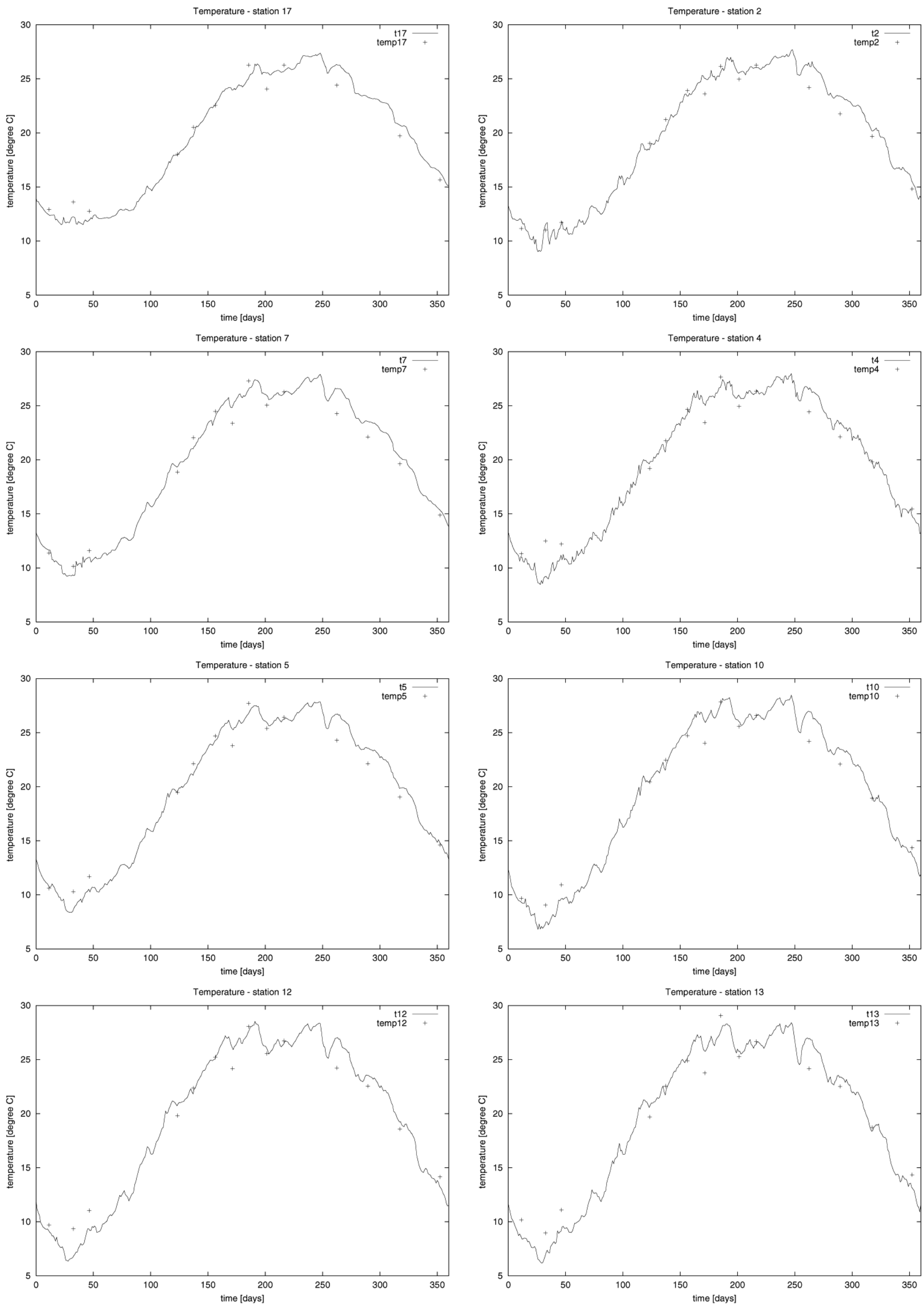

FIGURE 7 Results for the temperature, with the solar radiation data reduced in the summer period.

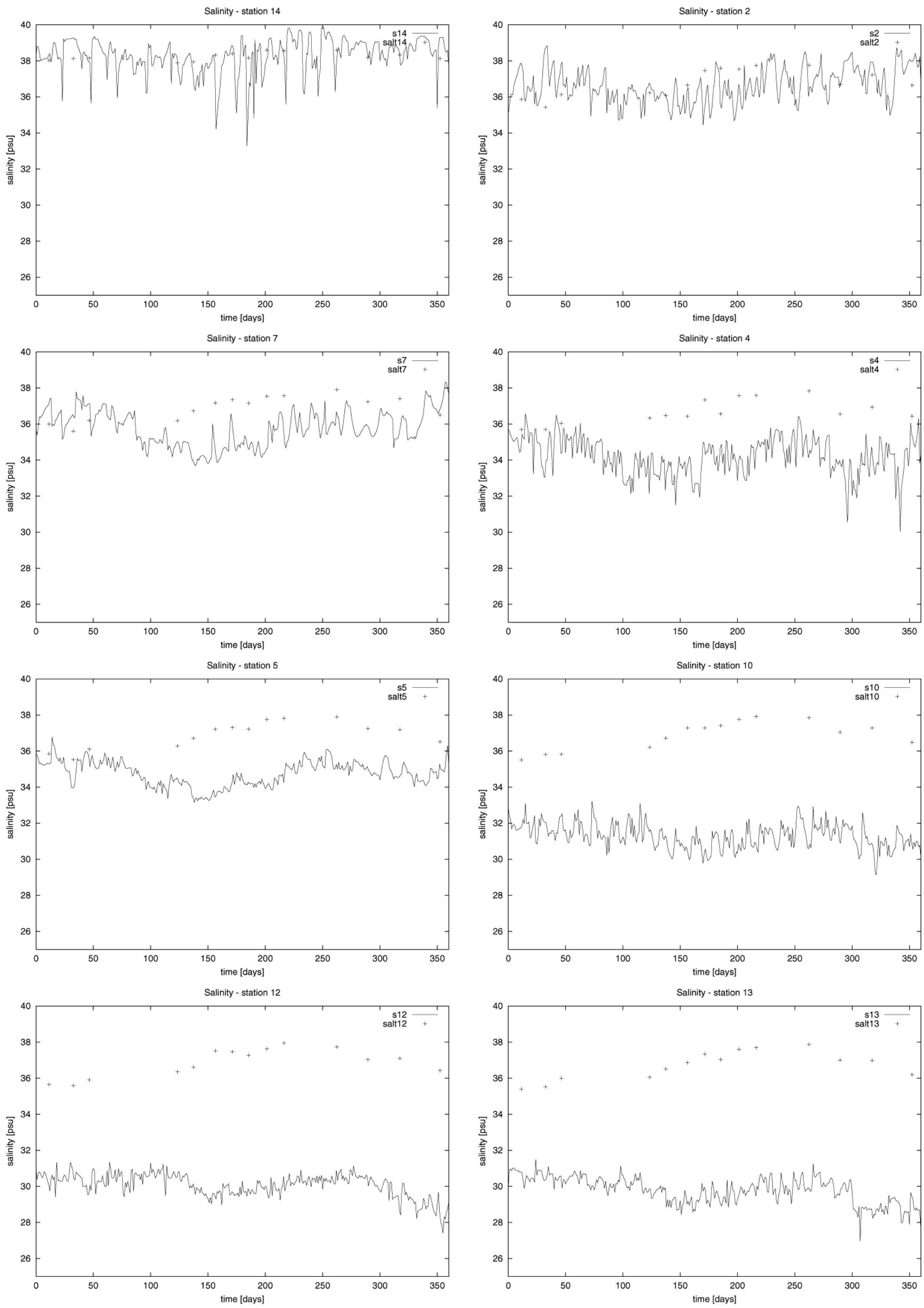

FIGURE 8 Results of the reference simulation for the salinity.

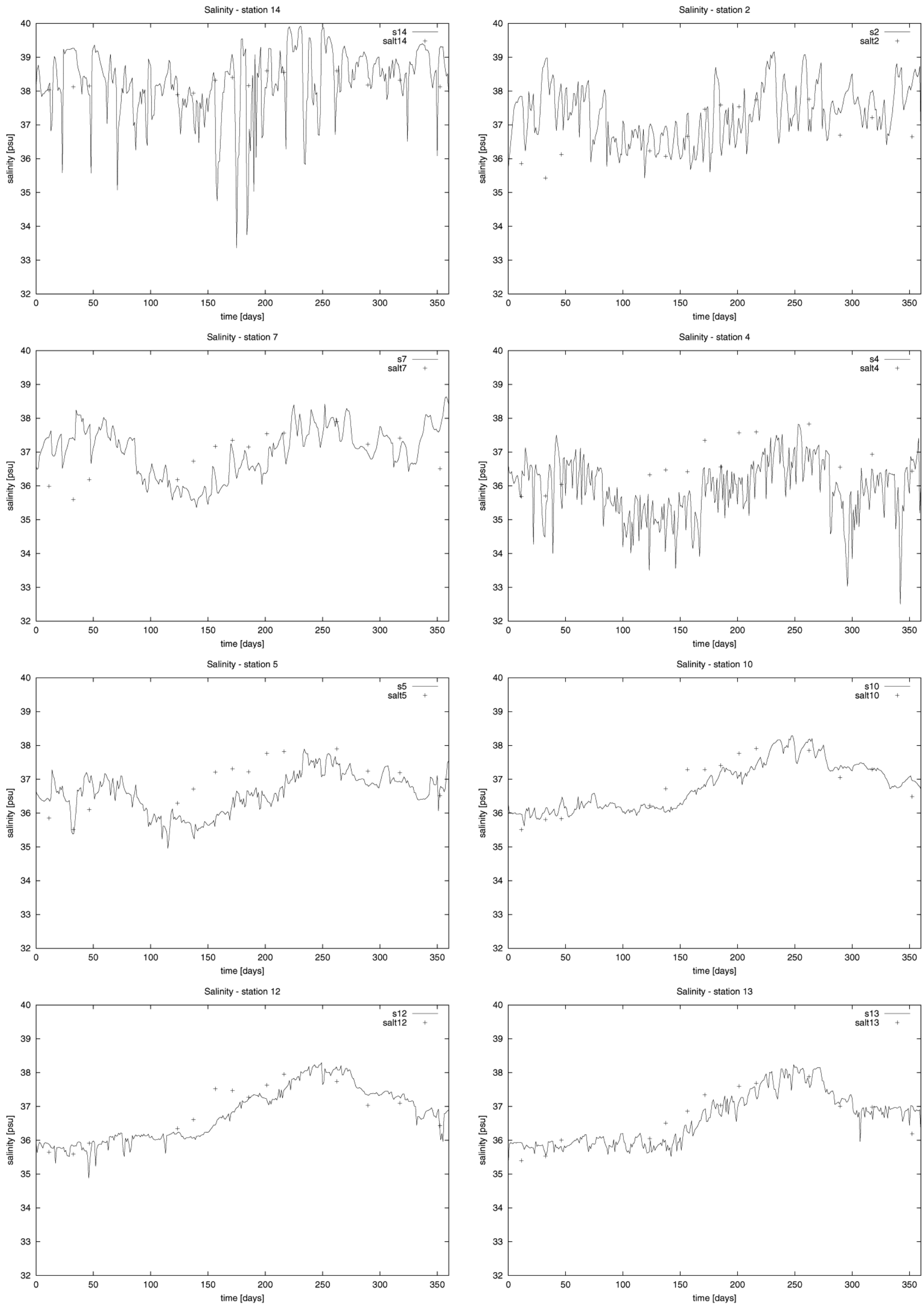

FIGURE 9 Results for the salinity, after the sensitivity analysis and the calibration.

There might be two causes of this behavior. One might be that the exchange rate between the Mar Piccolo and the Mar Grande is underestimated, and therefore the salinity of the Mar Piccolo remains too low. The other explanation for this discrepancy might be an overestimation and/or underestimation of some input data of the model.

As already pointed out in the Section 3.1, the exchange rates between the two basins are already at its maximum. The bottom friction parameter is not influencing the exchange rates too much and enhancing the stress of the wind by a factor of 2 does not improve the exchanges significantly. In Scroccaro *et al.* (2002b) it was found that none of the above-mentioned processes could raise the salinity in the Mar Piccolo by an evident amount.

It is therefore worthwhile looking at the boundary conditions that are imposed at the Mar Piccolo. Table II presents the comparison between two estimates of the fresh water spring inflows of the Mar Piccolo, provided by the Biology Department of Bari University and by the Istituto Talassografico of CNR of Taranto. It is noteworthy to point out the great uncertainty on the inflow of the citro Le Kopre. Furthermore, the seasonal variation of all the discharges is not known and might influence the results.

It has also to be stressed that the meteorological station is not inside the Mar Piccolo, and therefore the values of wind, humidity, and rain-evaporation might be a little bit different from their actual values. Moreover, the only measurements of discharges and salinity of the fresh water springs refer to studies and estimations in the 1960–1970s (Stefanon and Cotecchia, 1969), whereas the submarine springs are a phenomenon in continuous evolution that may strongly change during the years. Unluckily the bibliography on this subject is still rather scarse and not recent.

Taking into account the high amount of humidity present in the air, the evaporation data were enhanced by 20% during summer time. After many sensitivity tests the discharge of the citro Le Kopre, about which there is great uncertainty (see Tab. II), and Ajedda channel were reduced by 50% (see Scroccaro *et al.*, 2002b). The results of this simulation can be seen in Fig. 9.

With these modifications the model reproduces reasonably well the temporal and spatial variability of the data collected during the field campaign. For this simulation, the root mean square error was equal to 0.85 psu, while in the first experiment it was 3.76 psu. It is evident that the model results are very sensitive to variations of these factors and that the knowledge of their magnitude and seasonal fluctuations would be extremely important for the modeling of the Taranto Sea.

Figure 10 shows two instantaneous plots of the salinity field in the Taranto Sea, for 20 February 2000 (top panel) and 30 July 2000 (bottom panel). Along the coast the influence of the fresh water inflows are evident through lower values of salinity (darker colors), in particular the citro Galeso in the First Seno and the Ajedda channel in the Second Seno. The action of the water pump of ILVA can be seen in the First Seno, also. In the Mar Grande the Acquedotto discharges stand out near the stations 17 and 14 and are dispersed along the coast.

The two maps describe the salinity spatial variability during the year. Differences between the Mar Grande and the Mar Piccolo, and between the First Seno and the Second Seno of the Mar Piccolo can be observed. In the Mar Grande the salinity values are quite homogeneous both in winter and in summer. In the Mar Piccolo the situation greatly changes, especially in the Second Seno where the mean average salinity is definitely lower in winter (about 1.5–2.0 psu).

This behavior may be due, as explained above, to the effect of evaporation and to seasonal variations in the discharge values of the rivers and citri, stronger during the summer period. These effects are much less pronounced in the Mar Grande because the hydrodynamic exchange with the sea is higher and therefore the salinity fields are dominated by the sea water properties.

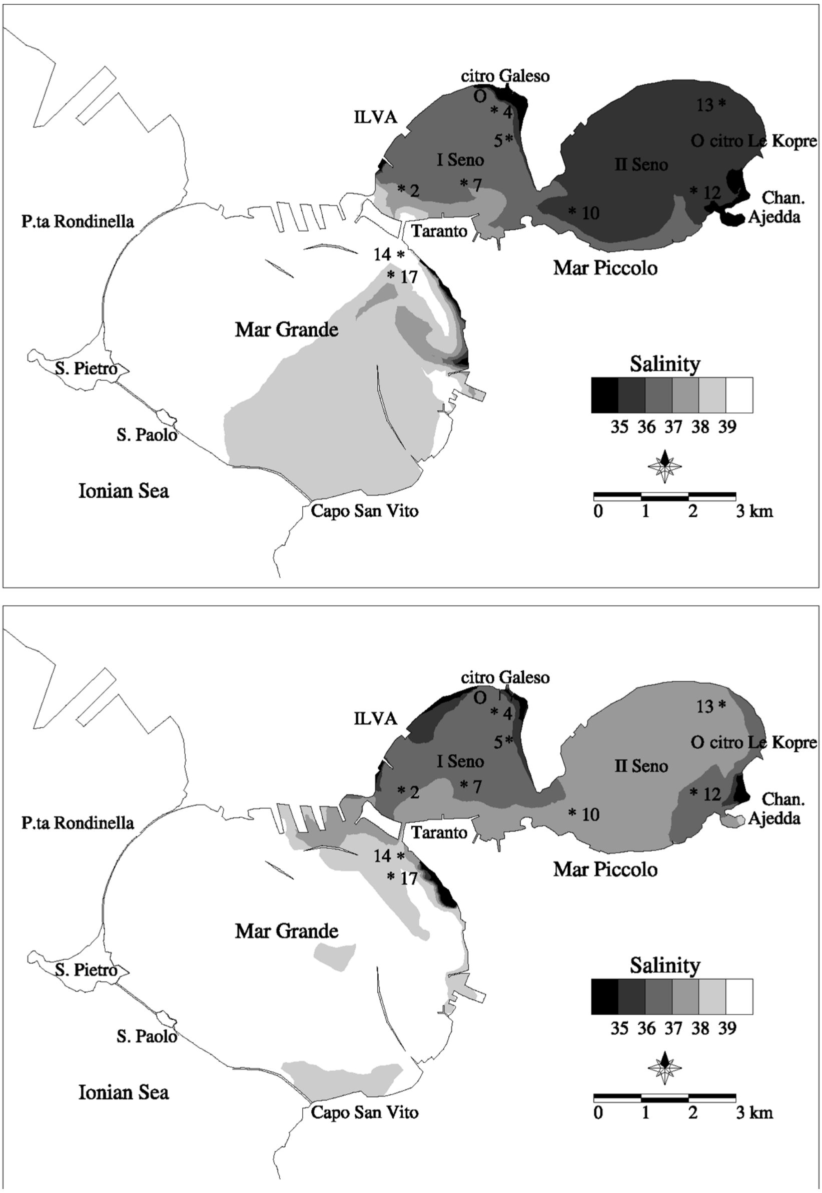

FIGURE 10 Instantaneous representations of the salinity field. Top: 20 February 2000. Bottom: 30 July 2000.

4 CONCLUSIONS

In this article a FE model, developed at CNR-ISMAR in Venice, has been applied to the Taranto Sea to simulate the hydrodynamic circulation, the temperature, and salinity behavior for the year 2000.

The model SHYFEM has been successfully applied to other coastal lagoons, in particular to the Venice lagoon, the Orbetello lagoon, and the Cabras lagoon. The model is a semi-implicit 2D FE model, especially suited for shallow, vertically well mixed basins.

Tide, wind, and inflows have been prescribed as forcings for the circulation. The salinity has been modeled taking into account the transport and diffusion processes and the rain-evaporation contribution. For the computation of temperature, the main physical processes that involve the exchange of heat fluxes between the atmosphere and the sea water have been considered.

Experimental data, collected by local research organizations during 2000–2001 *in situ* campaigns were used to calibrate and validate the model. The results show a good agreement between the computed results and the available measurements. Comparing the final results of the model to the corresponding data collected by the Istituto Talassografico of Taranto, a root mean square error equal to 1.37 °C has been found for the temperature. The value of the root mean square error for the salinity is of 0.85 psu.

As shown above, the salinity values depend crucially on the fresh water inflows and evaporation but are much less sensitive to the factors that influence the exchange rates between the Mar Grande and the Mar Piccolo. Therefore, the uncertainty of the results may be due to the introduction of some estimated data as forcing of the model, in particular for the fresh water springs inflow (see Tab. II).

The final results can be considered satisfactory, making the model a useful tool for the study of the physical and chemical processes in the Taranto Sea. Improvements could be obtained with the availability of salinity, temperature, and current measurements at the open boundaries.

The continuation of this study will be the application of a water quality model to study the eutrophication processes in the Taranto Sea.

Acknowledgements

The work has been carried out in the framework of the SPICAMAR project, as collaboration between ISMAR-CNR of Venice and Physics Department, University of Bari.

The authors wish to thank CoNISMa (Prof. A. Tursi) and Prof. L. Guerriero of Physics Department, University of Bari for the funding that enabled the study with the mathematical model SHYFEM. Special thanks to: Servizi Tecnici Nazionali, Biology Department, University of Bari, Istituto Meteorologico L. Ferrajolo of Taranto and Istituto Talassografico CNR of Taranto for the availability of the experimental data.

The authors also want to thank the unknown reviewers for the useful comments and suggestions that have helped to improve the quality of the article.

References

Alabiso, G., Cannalire, M., Ghionda, D., Milillo, M., Leone, G. and Caciorna, O. (1997). Particulate matter and chemical–physical conditions of an inner sea: The Mar Piccolo in Taranto. A new statistical approach. *Marine Chemistry*, **58**, 373–388.

Benincasa, F., Maracchi, G. and Rossi, P. (1991). *Agrometeorologia*. Patron Editore.

Cardellicchio, N., Annichiarico, C., Leone, G. *et al.* (1991). I mari di Taranto: problematiche di impatto ambientale. *Atti della Società italiana di Ecologia*, **12**, 769–775.

Cavallo, R. A., La Torre, F. and De Filippis, M. (1994). Valutazione dell'inquinamento del Mar Piccolo di Taranto: parametri microbiologici e indici biologici. *Biological Mar. Medit.*, **1**, 271–272.

Ferrarin, C. and Umgiesser, G. (2003). Hydrodynamic modeling of a coastal lagoon: The Cabras lagoon in Sardinia, Italy. *Ecological Modeling* (in press).

Pastore, M. (1993). Mar Piccolo. Nuova Eolitrice Apulia, Martina Franca, Taranto.

Scroccaro, I., Di Bitetto, M. and Umgiesser, G. (1999). Sensibility analysis of the circulation in the Orbetello lagoon. CNR-ISDGM, Venice, *Technical Report no. 228*, pp. 1–39.

Scroccaro, I., Di Bitetto, M. and Umgiesser, G. (2001). Sensibility analysis of the circulation in the Orbetello lagoon – Part 2. CNR-ISDGM, Venice, *Technical Report no. 242*, pp. 1–34.

Scroccaro, I., Matarrese, R. and Umgiesser, G. (2002a). Sviluppo e applicazione di un modello agli elementi finiti al Mare di Taranto. Parte I – Idrodinamica. ISDGM-CNR, Venice, *Technical Report no. 254*, pp. 1–48.

Scroccaro, I., Matarrese, R., Umgiesser, G. (2002b). Sviluppo e applicazione di un modello agli elementi finiti al Mare di Taranto. Parte II – Temperatura e salinità. ISDGM-CNR, Venice, *Technical Report no. 255*, pp. 1–45.

Stefanon, A. and Cotecchia, F. (1969). Prime notizie sulle caratteristiche di efflusso e sulle modalità di investigazione delle sorgenti subacquee ai fini di una loro captazione. *Quaderni de La Ricerca Scientifica*, **58**, pp. 165–195.

Strusi, A. and Pastore, M. (1975). Osservazioni idrografiche del Mar Grande e nel Mar Piccolo di Taranto. Campagna 1970–71. Oebalia I, 1–64.

Tursi, A., Piscitelli, G., Gherardi, M. and Matarrese, A. (1981). Aspetti ecologici del porto di Taranto (Mar Grande). Oebalia IV, 41–78.

Umgiesser, G. (1986). A model for the Venice lagoon. *Master thesis*, University of Hamburg.

Umgiesser, G. (1997). Modelling the Venice Lagoon. *International Journal of Salt Lake Research*, **6**, 175–199.

Umgiesser, G. (2000). Modeling Residual currents in the Venice Lagoon. *Interactions between Estuaries*, *Coastal Seas and Shelf Seas*, Terrapub, Tokyo, pp. 107–124.

Umgiesser, G. and Bergamasco, A. (1993). A staggered grid finite element model of the Venice Lagoon. in Morgan, K., Ofiate, E., Periaux, J. and Zienckiewicz, O. C. (eds.), *Finite Elements in Fluids.* Pineridge Press, pp. 659–668.

Umgiesser, G. and Bergamasco, A. (1995). Outline of a Primitive Equations Finite Element Model. In: Rapporto e Studi, Vol. XII. Istituto Veneto di Scienze, Lettere ed Arti. Venice, pp. 291–320.

Umgiesser, G., Melaku Canu, D., Solidoro, C. and Ambrose, R. (2003). A finite element ecological model: A first application to the Venice Lagoon. *Environmental Modelling and Software*, **18**, 131–145.

Vatova, A. (1972). Osservazioni fisico chimiche periodiche nel Mar Grande e Mar Piccolo di Taranto (1962–1969). *Bollettino Pesca Piscicoltura Idrobiologia*, **XXVII**(I), 43–79.

Zampato, L., Umgiesser, G. and Peron, F. (1998). Sviluppo di un modello di scambio termico all'interfaccia acqua-aria nella laguna di Venezia. ISDGM-CNR, Venice, *Technical Report no. 221*, pp. 1–33.